Multi-diagnostic characterization of geodesic acoustic modes in the TCV tokamak

Z. Huang[1], C.A. de Meijere[1], S. Coda[1], L. Vermare[2], T. Vernay[1], V. Vuille[1], S. Brunner[1], J. Dominski[1], P. Hennequin[2], A. Kraemer-Flecken[3], G. Maimbourg[4], G. Merlo[1], L. Porte[1], L. Villard[1]

[1] *CRPP, EPFL, Association EURATOM-Confédération Suisse, Lausanne, Switzerland*
[2] *Ecole Polytechnique, LPP, CNRS Palaiseau, France*
[3] *Forschungszentrum Jülich GmbH, EURATOM-Assoziation, Jülich, Germany*
[4] *Ecole Normale Supérieure de Cachan, France*

Introduction

The geodesic acoustic mode (GAM) is a finite-frequency oscillation of the turbulence-driven zonal-flow family [1], which is believed to be a key element in the self-organization of turbulence and in the regulation of turbulent transport through the shear-decorrelation mechanism [2]. The GAM is a $n = 0$, $m = 0$ electric potential pertubation, coupled by toroidal effects with a $n = 0$, $m = 1$ pressure perturbation. Recently, a $n = 0$, $m = 2$ magnetic perturbation caused by the GAM has also been predicted by theory [3].

The GAM has recently been studied experimentally in the TCV tokamak with multiple diagnostics, including phase-contrast imaging (PCI), magnetic probes, correlation ECE and Doppler backscattering. Uniquely, the mode is observed simultaneously by all these systems. In particular, we report on the first full characterisation of the magnetic component of the turbulence-driven GAM. This also permits the first unambiguous determination of the axisymmetry of the mode from a complete, multi-point toroidal array. In parallel, gyrokinetic simulations have been performed with the global particle-in-cell code ORB5 [4] and directly compared with experimental measurements.

Multi-diagnostic measurements of GAMs in TCV

This paper presents a unique, correlated multi-diagnostic experimental characterisation of the GAM in the TCV tokamak (major and minor radius 0.88 and 0.25 m, respectively, vacuum magnetic field 1.5 T) [5]. The GAM has been detected in Ohmic as well as electron-cyclotron-heated plasmas, in a wide variety of plasma shapes, and for varying safety factor and collisionality.

The theoretically expected [3] magnetic component of the turbulence-driven GAM was characterised for the first time, using the poloidal and toroidal magnetic probe arrays [6] on TCV. Figure 1(a) shows the power spectrum of the toroidally symmetric ($n = 0$) and non-symmetric ($n \neq 0$) components of the magnetic field fluctuations, measured on the high field side (HFS)

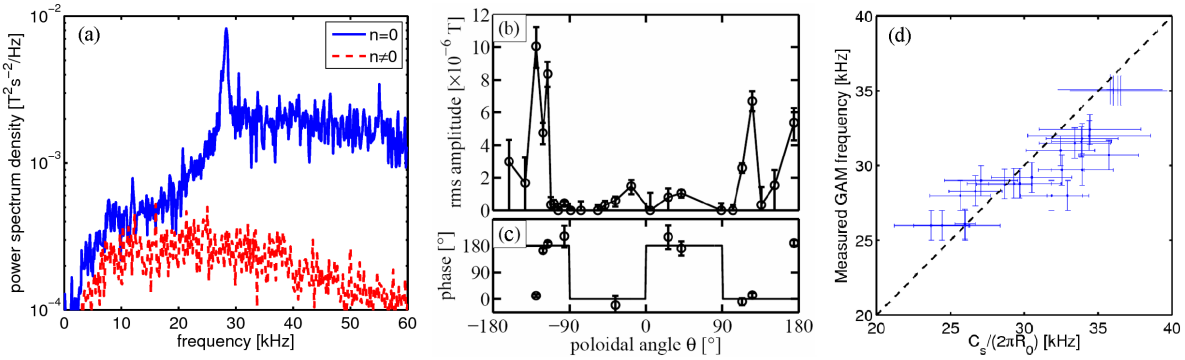

Figure 1: (a) Auto-power spectrum of GAM magnetic component. (b) RMS GAM amplitude as measured by the poloidal array of magnetic probes. (c) Cross-phase with the $n = 0$ signal. (d) Frequency scaling of the GAM with the ion sound speed.

and 35 cm above the magnetic axis. The GAM is evident as a peak at 28 kHz in the $n = 0$ spectrum, which yields an unambiguous determination of the axisymmetry. Figs. 1(b) and (c) show the root-mean-square (RMS) amplitude and cross-phase with respect to the toroidal symmetric component of the GAM as a function of poloidal angle θ, which is the geometrical angle with respect to the magnetic axis for each probe. The presence of antinodes and π phase jumps indicates that the GAM is dominated by a $m = 2$ standing wave sturcture in the poloidal plane, as predicted by theory. Fig. 1(d) shows that the frequency of the GAM roughly follows the expected c_s/R scaling law, c_s being the ion sound speed. This fact, together with the observed toroidal axisymmetry, indicates that the mode under consideration is indeed a GAM.

The density component of the GAM is measured with a newly installed tangential phase contrast imaging (TPCI) diagnostic [7, 8, 9]. The diagnostic measures line-integrated electron density fluctuations, and spatial resolution is added from the tangential geometry and spatial filtering. For a radial mode such as the GAM, the measurement of TPCI is localised at the point where the chords are tangent to the magnetic flux surfaces. By shifting the plasma column vertically in the vacuum vessel, the radial distribution of the GAM can be resolved (Fig. 2(e,f)). It has measurable amplitude for $\rho_\Psi > 0.65$, with the peak located near the last closed flux surface, at $\rho_\Psi \cong 0.95$ (Fig. 2(b)). Fig. 2(a) shows that the GAM frequency is around 28 kHz, which is coherent with the toroidal symmetric component from the magnetic probe measurement. The frequency is constant in the entire radial range of existence of the mode, over which the ion sound speed varies by a factor 1.7, which implies that it is a global GAM eigenmode [10]. The complex coherence function at the GAM frequency is also calculated to study the radial correlation structure (Fig. 2(c,d)), showing that it is an outward propagating mode, with radial wavenumber between 1.7 and 2.1 cm^{-1}. Normalising these wave-numbers to ρ_s (the ion sound

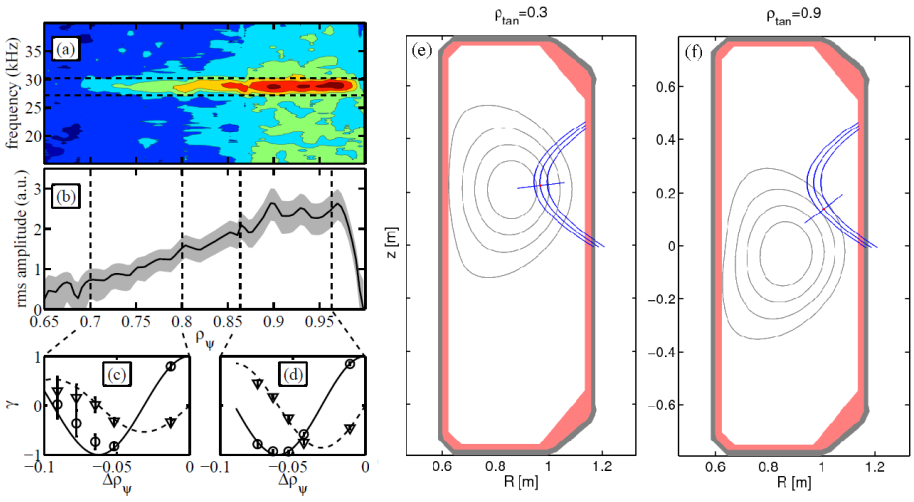

Figure 2: (a) Auto-power spectrum of density fluctuations. (b) RMS GAM amplitude as measured by TPCI. (c,d) Real (○) and imaginary (∇) parts of the complex coherence at the GAM frequency. (e,f) Poloidal projection of the beam path and measurement position in the TCV vessel

Larmor radius) for $\rho_\Psi = 0.95$ yields values of $k\rho_s$ between 0.4 and 0.5.

The heterodyne Doppler backscattering system used in these studies includes a tuneable instrument between 50 and 75 GHz from LPP [11] and a 45 GHz instrument from FZJ, coupled to a monostatic steerable antenna. The propagation velocity of associated $E \times B$ flow close to the last closed flux surface is obtained from the measured Doppler shift; after subtraction of the dc velocity, the only statistically significant feature of the power spectrum of the propagation velocity is a peak at the GAM frequency, which is coherent with the TPCI and magnetic signals. In addition, a correlation elecron cyclotron emission (CECE) diagnostic is used to measure the radiative temperature component. The GAM is visible as a modest peak at the same frequency found by other diagnostics [12]. However, the diagnostic can be affected by both density and temperature fluctuations owing to low optical depth. Further work is underway to separate the two.

The GAM is coherently observed by all the diagnostics, as shown by Fig. 3. However, there are still some discrepancies. The radial wavenumber is measured to be between 1.7 to 2.1 cm^{-1} from TPCI, whereas a value 0.9 cm^{-1} is inferred from CECE. TPCI also shows that the GAM is always predominatly propagating outward, while CECE gives different propagation directions at different locations.

Modeling of GAMs in TCV

Gyrokinetic simulations have been performed with the global nonlinear particle-in-cell code ORB5 [4] and directly compared with experimental measurements. Collisions and electromag-

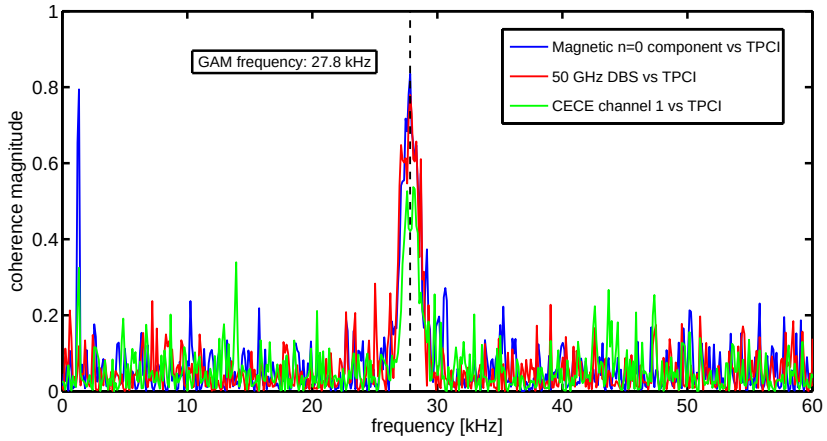

Figure 3: Magnitude of complex coherence between the magnetic $n = 0$ component, 50-75 GHz Doppler backscattering, CECE channel 1 to central channel of TPCI

netic effects are neglected and the plasma is assumed to consist solely of deuterium. Turbulence in the simulation is driven mainly by the trapped-electron-mode (TEM) instability. Various modified density profiles from the TCV experimental data were used in the simulation, but keeping the same temperature profile. In all cases GAM activity is evident in coherent oscillations of the flux-surface averaged electric potential for $\rho > 0.7$. The mode is outward propagating, with frequency 33 kHz, radial wave-number 2.3 cm^{-1}, and amplitude steadily increasing in the interval $0.7 < \rho_\Psi < 0.85$ (the outermost radius resolved by the simulation). The poloidal structure of the density fluctuations is found to be dominated by $m = 1$. These simulation results are in semi-quantitative agreement with the exprimental observations in TCV.

This work was supported in part by the Swiss National Science Foundation.

References

[1] Diamond, P. H., Itoh, S.-I., Itoh, K., et al. *Plasma Physics and Controlled Fusion* **47**, R35 (2005).

[2] Diamond, P. H. and Biglari, H. *Physical Review Letters* **65**, 2865 (1990).

[3] Wahlberg, C. *Plasma Physics and Controlled Fusion* **51**, 085006 (2009).

[4] Vernay, T., Brunner, S., Villard, L., et al. *Physics of Plasmas* **17**, 122301 (2010).

[5] Hofmann, F., Lister, J. B., Anton, W., et al. *Plasma Physics and Controlled Fusion* **36**, B277 (1994).

[6] Moret, J.-M., Buhlmann, F., Fasel, D., et al. *Review of Scientific Instruments* **69**, 2333 (1998).

[7] Marinoni, A., Coda, S., Chavan, R., et al. *Review of Scientific Instruments* **77**, 10E929 (2006).

[8] de Meijere, C. A. PhD thesis 5610, Ecole Polytechnique Fédérale de Lausanne (2013).

[9] Coda, S., de Meijere, C. A., Huang, Z., et al. this conference (P1.169).

[10] Itoh, K., Itoh, S.-I., Diamond, P. H., et al. *Plasma and Fusion Research* **1**, 037 (2006).

[11] Vermare, L., Hennequin, P., Gurcan, O. D., et al. *Nuclear Fusion* **52**, 063008 (2012).

[12] Vuille, V., Porte, L., Coda, S., et al. this conference (P2.176).